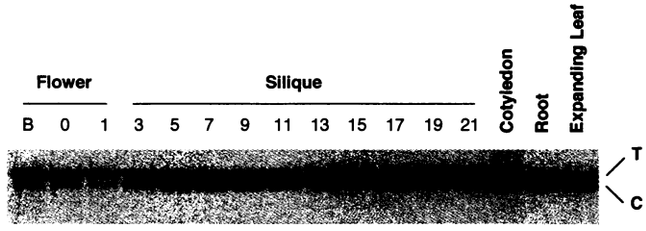

Fig. 4. Competitive RT-PCR analyses of *SSE1* expression profiles. RNA was isolated from flowers before (B), on the day of (0), or 1 day after pollination (1); from siliques 3 to 21 days after pollination; from cotyledons of 2-day-old seedlings; and from expanding rosette leaves and roots. An equal amount of competitor cDNA template was included in each reaction. The *SSE1* target (T)-to-competitor (C) cDNA ratios reflect the relative expression levels of the *SSE1* gene (*17*).

References and Notes

1. D. J. Bewley and M. Black, *Seeds: Physiology of Development and Germination* (Plenum, New York, ed. 2, 1994), chap. 1; A. Vitale and R. Bollini, in *Seed Development and Germination*, J. Kigel and G. Galili, Eds. (Dekker, New York, 1995), pp. 73–102; M. Miquel and J. Browse, in *ibid.*, pp. 169–193.
2. S. G. Mansfield and L. G. Briarty, *Can. J. Bot.* **70**, 151 (1992).
3. The cDNA of the *Arabidopsis* prohibitin gene *Atphb1* (L. Sun and H. M. Goodman) in an antisense orientation was inserted into pBI121 (Clontech) between the Sac I and Bam HI sites to replaced the β-glucuronidase coding region. One of 49 C24 transgenic lines showed the shrunken seed phenotype (*sse1*). Northern (RNA) blot analysis with an *Atphb1* cDNA bottom-strand probe showed that the *Atphb1* mRNA level in this line is similar to that of the wild type.
4. The transgenic line was propagated by self-pollination for four generations (to T5). Ten round seeds were grown from each generation, and each produced 90% shrunken seeds.
5. T2 plants derived from round seeds were crossed reciprocally to wild-type C24 plants. All F_1 seeds were round. The numbers of shrunken/round F_2 seeds in six single siliques were 11/39, 15/36, 12/39, 10/42, 11/36, and 10/40; these numbers are consistent with an expected segregation ratio of 1:3 ($\chi^2 = 0.64$, $P > 0.1$).
6. Two hundred and sixty F_3 seed families were obtained from individual F_2 round seeds; 180 families segregated for both the shrunken and kanamycin-resistant (conferred by the T-DNA) phenotypes, whereas the other 80 showed neither phenotype.
7. A 136–base pair (bp) genomic DNA fragment flanking the T-DNA was isolated by the thermal asymmetric interlaced–polymerase chain reaction (*20*). A 17-kb genomic fragment isolated from a λ-FIXII *Arabidopsis* C24 genomic library (L. Sun and H. M. Goodman) was used as a probe to screen an *Arabidopsis* cDNA library [M. Minet, M.-E. Dufour, F. Lacroute, *Plant J.* **2**, 417 (1992)]. The two *SSE1* cDNA clones have identical 5′ ends, and both include the stop codon. The 3′ polyadenylation site was determined by 3′ RACE (rapid amplification of cDNA ends) PCR. Newly released bacterial artificial chromosome (BAC) sequences revealed that *SSE1* is within the BAC clones F17K2 and F4I18 (GenBank accession numbers AC003680 and AC004665). The SSE1 protein predicted by the open reading frame differs from the F17K2.22 hypothetical protein as a result of discrepancies between the predicted and the actual splicing sites.
8. DNA was isolated from single embryos after removal of the seed coat, which has the same genotype as the parent.
9. F_1 seeds were obtained from reciprocal crosses between a round seed–derived T3 plant and a wild-type plant. Their genotypes were examined to determine the genotypes of the gametes from the T3 plant. The wild-type allele was present in 3 out of 39 eggs and 0 out of 51 sperms; the rest of the gametes carried the mutant allele. Therefore, the T4 progeny would be either homozygous *sse1* (36/39 = 92%) or heterozygous (3/39 = 8%).
10. The *SSE1* cDNA was fused with the 35S promoter (*35SP*) and the nopaline synthase 3′ region (*NOS* 3′). The *35SP-SSE1-NOS*3′ cassette was subcloned into the Kpn I site of the pLVN19R binary vector to make the pLVN19R-*SSE1* construct. T3 plants from round seeds were vacuum-infiltrated with *Agrobacterium tumaficiens* strain GV3101 [N. Bechtold, J. Ellis, G. Pelletier, *C. R. Acad. Sci. Paris Life Sci.* **316**, 1194 (1993)] carrying pLVN19R-*SSE1*. Genotypes of seven methotrexate-resistant transgenic plants were determined by PCR, and six were homozygous *sse1*. Four transgenic *sse1* plants were fertile and produced complemented T2 seeds at 67 to 87%.
11. G. A. Eitzen, R. K. Szilard, R. A. Rachubinski, *J. Cell Biol.* **137**, 1265 (1997).
12. V. I. Titorenko, D. M. Ogrydziak, R. A. Rachubinski, *Mol. Cell. Biol.* **17**, 5210 (1997).
13. V. I. Titorenko and R. A. Rachubinski, *ibid.* **18**, 2789 (1998).
14. L. J. Olsen and J. J. Harada, *Annu. Rev. Plant Physiol. Plant Mol. Biol.* **46**, 123 (1995).
15. M. J. Chrispeels, *ibid.* **42**, 21 (1991); C. Sarmiento, J. H. Ross, E. Herman, D. J. Murphy, *Plant J.* **11**, 783 (1997).
16. A. H. C. Huang, *Plant Physiol.* **110**, 1055 (1996).
17. After deoxyribonuclease treatment, 1 μg of RNA was reverse transcribed in a 20-μl reaction, with 0.4 μM of the *SSE1*-specific primer FP15R (5′-GGCAATATTCTTCCGTTGC-3′). Subsequently, 1 μl of the reverse-transcription mixture and 5×10^{-21} mol of competitor cDNA were used in each 20-μl PCR reaction. The competitor cDNA is identical to the *SSE1* cDNA (designated target cDNA) except for a 95-bp internal deletion from the Eco RI to the Nco I site. The primers FP7 (5′-AAAAATGGAACTACATTATTCTC-3′) and FP14R (5′-ATAAGTAAAACGCTTAACCTHC-3′) amplify 814- and 719-bp fragments, respectively, from the target and the competitor cDNAs. The ratio of the two PCR products reflects the relative amount of *SSE1* cDNA (or mRNA) in each sample [P. D. Siebert and J. W. Larrick, *Nature* **359**, 557 (1992)].
18. D. W. Meinke, L. H. Franzmann, T. C. Nickle, E. C. Yeung, *Plant Cell* **6**, 1049 (1994).
19. Z. Chen, H. Ilarslan, R. G. Palmer, R. C. Shoemaker, *Am. J. Bot.* **85**, 492 (1998).
20. Y.-G. Liu, N. Mitsukawa, T. Oosumi, R. F. Whittier, *Plant J.* **8**, 457 (1995).
21. Mature wild-type C24 and once-backcrossed *sse1* seeds were used. *sse1* seeds were imbibed in water for 20 min before processing. Seeds were cut into halves and fixed in 2.5% glutaraldehyde–0.1 M cacodylate (pH 7.2), post-fixed in 1% osmium tetroxide, dehydrated in an ethanol series, and embedded in Spurr's resin. Thin sections were stained with uranyl acetate and observed under a transmission electron microscope.
22. J. Kyte and R. F. Doolittle, *J. Mol. Biol.* **157**, 105 (1982).
23. *SSE1* cDNA was cloned into the Eco RI site of a *Y. lipolytica* shuttle vector pTc3 between the promoter and the terminator regions of *Y. lipolytica* thiolase gene. Ura$^+$ transformants of *pex16-1* and *P16KO-8A* were obtained (*11*).

24. We thank W. Fowle for assistance with electron microscopy, and J. Nardone, Y. Kovtun, and L. Zhou for critical reading of the manuscript. This work was supported by a grant from Hoechst AG to H.M.G.

15 October 1998; accepted 5 March 1999

Regulation of Maternal Behavior and Offspring Growth by Paternally Expressed *Peg3*

L.-L. Li,[1]* E. B. Keverne,[2] S. A. Aparicio,[1] F. Ishino,[3] S. C. Barton,[1] M. A. Surani[1]†

Imprinted genes display parent-of-origin–dependent monoallelic expression that apparently regulates complex mammalian traits, including growth and behavior. The *Peg3* gene is expressed in embryos and the adult brain from the paternal allele only. A mutation in the *Peg3* gene resulted in growth retardation, as well as a striking impairment of maternal behavior that frequently resulted in death of the offspring. This result may be partly due to defective neuronal connectivity, as well as reduced oxytocin neurons in the hypothalamus, because mutant mothers were deficient in milk ejection. This study provides further insights on the evolution of epigenetic regulation of imprinted gene dosage in modulating mammalian growth and behavior.

Maternal and paternal genomes contribute unequally to development (*1*) through the monoallelic expression of imprinted genes that affect embryonic and placental development, as well as behavior in mice (*2*). It is possible that complex behavioral output of the central nervous system (CNS) might be a common function of a disparate group of neurally expressed imprinted genes such as *Mest* and *Peg3*. In this context, we showed previously that parthenogenetic (PG: duplicated maternal genome) and androgenetic (AG: duplicated paternal genome) cells contribute unequally to the formation of the CNS in chimeric mice (*3*). PG cells contribute more to the cortex and striatum, whereas AG cells contribute to the hypothalamus. The imprinted gene *Mest* of paternal origin is expressed in the hypothalamus and functions in regulating growth and maternal behavior

(*4*). Another paternally expressed gene, *Peg3*, of unknown function is expressed in a variety of embryonic meso-endodermal tissues, in the hypothalamus and the adult brain (*5*–*7*). The putative Peg3 protein contains 12 C_2H_2-type zinc-finger motifs and two proline or acidic amino acid–rich repeat domains (*5*, *6*), suggesting its involvement in DNA-binding and protein-protein interactions, respectively. Recently, *Peg3* (also known as *Pw1*) was implicated as a partner protein to TRAF2 (*8*) and in the tumor necrosis factor (TNF) signaling pathway.

To study the function of *Peg3* in vivo, we mutated the gene by insertion of a β*geo* selection cassette into its 5′ coding exon using gene targeting (Fig. 1A) (*9*). The heterozygous embryos that inherited the *Peg3*$^{\beta geo}$ mutation from the paternal germ line (designated +/–) showed no detectable wild-type *Peg3* mRNA (Fig. 1B) (*10*). However, they showed appropriate β-galactosidase (β-Gal) expression (*5*, *6*) (Fig. 1C). In adults, β-Gal expression was localized in the brain (Fig. 1D), pituitary, and adrenal medulla. The +/– mice were smaller (*11*) but otherwise fertile, healthy, and normal in their general behavior. As expected, maternal transmission of the mutation (designated –/+) had no phenotypic effects and showed no β-Gal activity throughout development (Fig. 1C). Thus, the mutant *Peg3*$^{\beta geo}$ locus was imprinted exactly as the endogenous wild-type locus.

A distinct behavioral phenotype became evident from interbreeding of +/– heterozygotes. Very few first litters (8%) of mutant mothers (+/–) grew to weaning age, compared with those nursed by wild-type females (83%). As the progeny from mutant females and wild-type males (+/– × +/+) also failed to survive, this suggested that the genotype of the father was not relevant for their survival. More importantly, as the progeny inherited the active paternal *Peg3* allele and the silent maternal *Peg3*$^{\beta geo}$ mutant allele, they should develop as normal adults. Their failure to thrive showed the existence of a maternal nurturing defect. Nevertheless, mutant females improved their nurturing ability by the third parturition because most of them (7 of 10, 70%) cared for their young, although they remained maternally impaired (see below).

Because the newborn rodents are deaf, blind, and immobile, the mother normally builds a nest, gathers her pups together, and keeps them warm by crouching over them. We found that the mutant primiparous mother failed to exhibit any of these maternal responses. To validate these observations, we first tested the response of the postpartum mothers toward three newborn pups (Fig. 2). Mutant mothers took 11 times longer to retrieve and 8 times longer to build a nest and, unlike wild-type mothers, never crouched over their pups in the 15 min of testing. The inability to find the pups was not a factor for the impaired maternal response, as the mutant mothers sniffed the pups as quickly as wild-type mothers (14.0 ± 5.4 s compared with 8.8 ± 4.2 s; $P > 0.1$).

The rapid onset of maternal behavior seen in postpartum females is induced by both the hormonal priming during pregnancy and the stimulus from contact with pups at parturition (*12*). Sensory exposure to pups can also induce maternal behavior in virgin females, although this response is less immediate (*13*). To determine whether the *Peg3*$^{\beta geo}$ mutation affects maternal behavior independently of pregnancy and parturition, we examined virgin and multiparous diestrus females for maternal behavior (Fig. 2). All of these mutants, with or without maternal experience, spent a significantly longer time than control animals

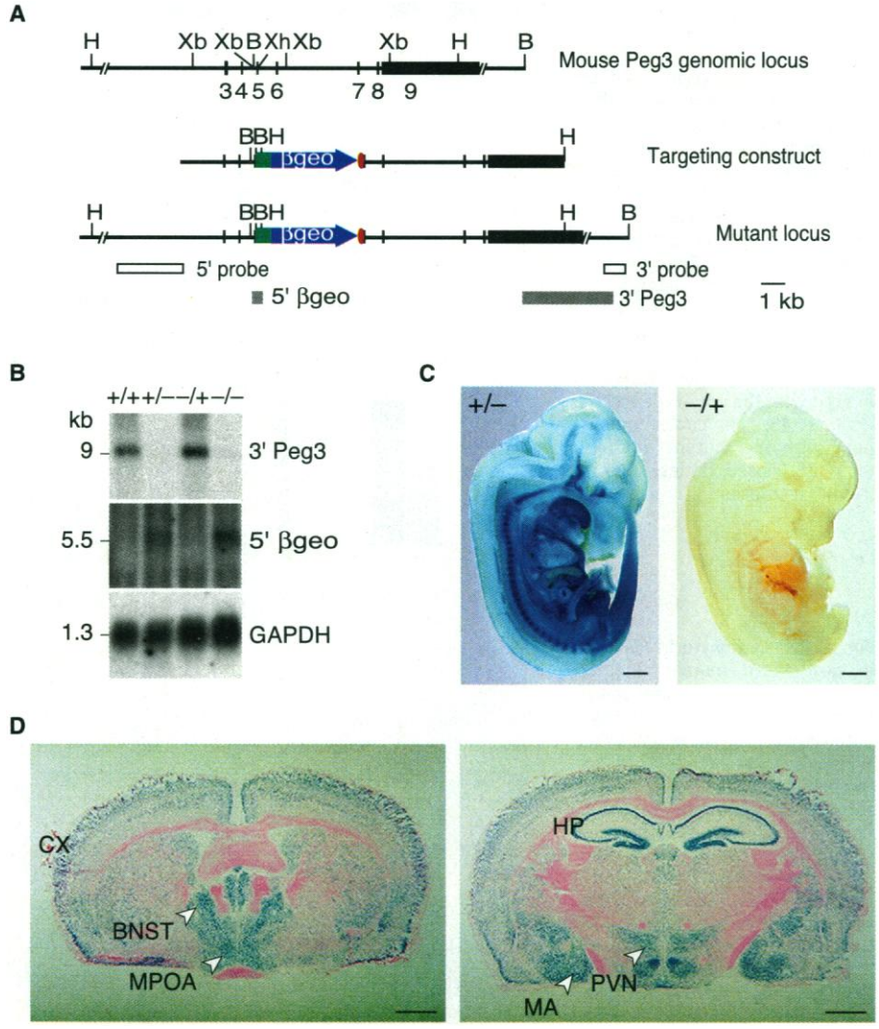

Fig. 1. Generation and characterization of *Peg3*$^{\beta geo}$ mutant mice. (**A**) The wild-type *Peg3* locus with its open reading frame spans from exon 3 to 9 (black boxes). The mutant *Peg3*$^{\beta geo}$ locus was generated by insertion of a β*geo* selection cassette containing an internal ribosome entry site (green box), *lacZ-neo* fusion gene (blue arrow), and SV40 polyadenylation (red oval) into exon 5. H, Hind III; B, Bgl II; Xb, Xba I; Xh, Xho I. Probes used for Southern and Northern blot analyses are shown as open and grey boxes, respectively. (**B**) Northern blot analysis of mRNA (2 μg/lane) from the wild-type (+/+), paternal heterozygote (+/–), maternal heterozygote (–/+), and homozygote (–/–) embryos at 12.5 dpc. GAPDH, glyceraldehyde-3-phosphate dehydrogenase. (**C**) β-Gal staining of sagittal planes of the +/– and –/+ embryos at 12.5 dpc (*23*). (**D**) β-Gal staining of coronal brain cryosections from the +/– adult mice. High expression was observed in the neuronal regions known to be crucial for maternal behavior (indicated by arrows) (*15*). CX, cortex; MPOA, medial preoptic area; PVN, paraventricular nucleus; MA, medial amygdala; BNST, bed nucleus of the stria; HP, hippocampus. Scale bars, 1.0 mm.

[1]Wellcome CRC Institute of Cancer and Developmental Biology, and Physiological Laboratory, University of Cambridge, Tennis Court Road, Cambridge CB2 1QR, UK. [2]Sub-Department of Animal Behavior, University of Cambridge, Madingley, Cambridge, UK. [3]Gene Research Center, Tokyo Institute of Technology, 4259 Nagatsuta-cho, Midori-ku, Yokohama 226, Japan.

*Present address: Columbia University, College of Physicians and Surgeons, Department of Genetics and Development, New York, NY 10032, USA.

†To whom correspondence should be addressed. E-mail: as10021@mole.bio.cam.ac.uk

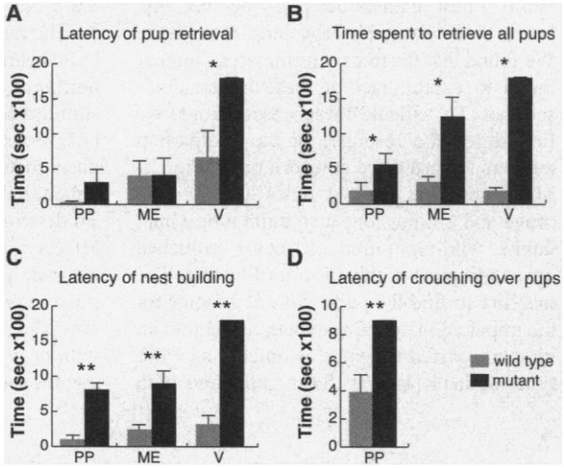

Fig. 2. Impaired maternal behavior in the *Peg3*$^{\beta geo}$mutant females (*24*). The wild-type (grey bars) and +/– mutant (black bars) primiparous postpartum (PP), multiparous diestrus (ME), and diestrus virgin (V) females were examined for maternal response toward pups (n = 6). (**A**) Latency of pup retrieval, (**B**) time spent to retrieve all pups, (**C**) latency of nest building, and (**D**) latency of crouching over pups were recorded. The data represent the mean ± SEM. *, $P <$ 0.05; **, $P <$ 0.01 by Mann-Whitney U test.

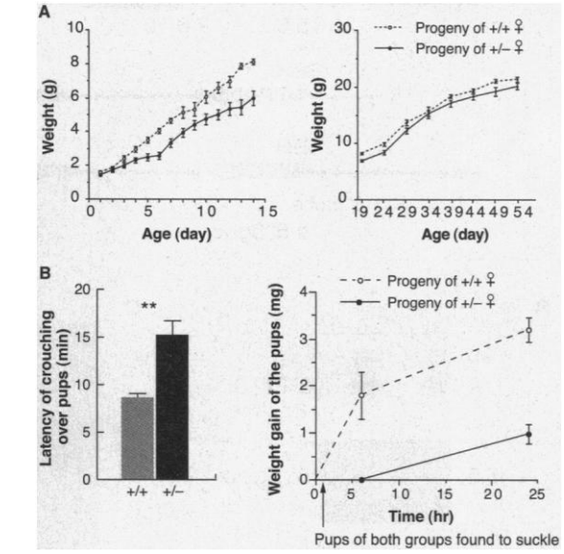

Fig. 3. Reduced weight gain in pups nursed by the mutant mothers. (**A**) Body weight (mean ± SEM) of progeny (n = 12) from +/+ female × +/+ male crosses (open circles) and of progeny (n = 12) from +/– female × +/+ male crosses (closed circles) before (left) and after (right) weaning. (**B**) (left) The latency of crouching behavior of the wild-type (grey bar) and +/– mutant (black bar) mothers (n = 6). (right) The weight gain observed in pups with the wild-type mothers (n = 46, open circles) and in pups with the mutant mothers (n = 26, closed circles) after a 2-hour separation.

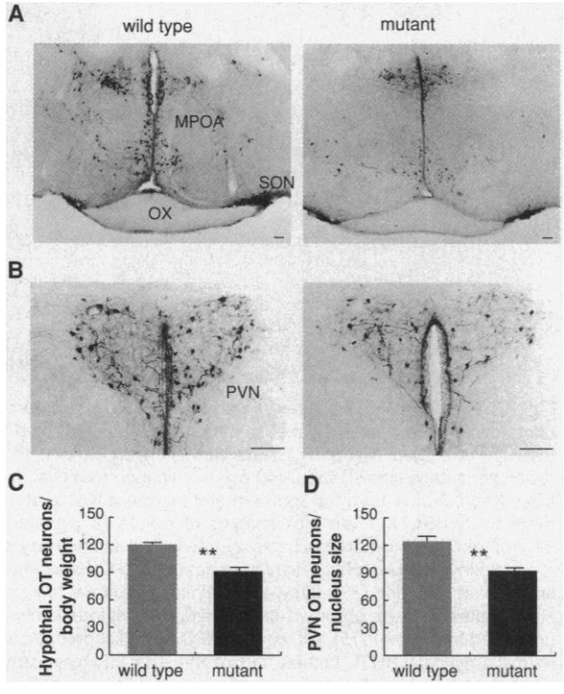

Fig. 4. Reduced oxytocin neurons in postpartum mutant females (*25*). Immunohistochemical staining of oxytocin neurons in the hypothalamus of postpartum wild-type and mutant females: (**A**) in the MPOA and supraoptic nucleus (SON) and (**B**) in the PVN. OX, optic chasma. Scale bars, 0.3 mm. (**C** and **D**) The number of oxytocin (OT) neurons in the hypothalamus (Hypothal.) relative to body weight and (C) in the PVN relative to the size of the nucleus (D), in the wild-type (grey bars) and mutant (black bars) females. The data are expressed as ±SEM. **, $P <$ 0.01.

in retrieving all the pups and in exhibiting nest-building activity. Thus, maternal behavior induced by pup exposure was also affected by the mutation.

The neural circuit responsible for maternal behavior is complex because it involves multisensory stimulation in the female after exposure to the pups. High levels of *Peg3* expression were present in the hypothalamic nuclei, including the medial preoptic area (MPOA), as well as in the medial amygdala, bed nucleus of the stria terminalis, hippocampus (see Fig. 1D), and olfactory bulb (*14*). Lesion analysis previously showed that several of these regions are crucial for maternal behavior (*15*). Thus, the neural expression pattern of *Peg3* is consistent with its role in regulating maternal behavior. However, no obvious structural anomalies were observed in the brain sections of the mutants, and β-Gal expression matched that of *Peg3* RNA in wild-type females. We also examined expression of the *fosB* gene in the hypothalamic MPOA area because it is activated rapidly by exposure of virgin females to pups (*16*). Furthermore, a null mutation of this *fosB* gene causes impaired maternal behavior in both postpartum and virgin females (*16*). However, our *Peg3*$^{\beta geo}$ mutant virgin females did show appropriate *fosB* induction in the MPOA after their exposure to pups, suggesting that the lack of maternal behavior is independent of *fosB* activation.

Despite the smaller litter size of *Peg3*$^{\beta geo}$ females, the surviving (nonmutant) progeny gained less weight compared with progeny of wild-type mothers during the first 3 weeks ($P <$ 0.002) (Fig. 3A, left). However, their weight did catch up after weaning (P = 0.7449) (Fig. 3A, right). The preweaning deficiency in weight gain could result from either impaired maternal response or a defect in lactation in the mutant females (or from both). To test this, we measured both maternal behavior and the weight gain by the pups after the separation of the mothers and pups for 2 hours (Fig. 3B). The mutant mothers were slower in adopting the crouching posture compared with wild-type mothers (15.3 min compared with 8.7 min; n = 6, $P <$ 0.004), but the pups of both groups attached to the nipples after 1 hour. In the control group, the pup's weight increased by 1.8 ± 0.5 and 3.2 ± 0.25 mg after 6 and 24 hours, respectively. By contrast, the pups suckled by the mutant mothers gained no weight after 6 hours and only 0.98 ± 0.2 mg after 24 hours ($P <$ 0.01). The reduced weight gain in the latter suggested a defect in lactation in the mutant mothers.

To determine the underlying cause of lactational defect, we first examined the mammary glands of the mutant mothers but found them to be histologically normal both at prepartum and postpartum. Next, we examined oxytocin neurons because milk ejection is controlled by oxytocin released from the

hypothalamic paraventricular (PVN) and supraoptic nuclei in response to the suckling stimulus; a mutation in the oxytocin gene abolishes milk ejection (*17*). We found that the postpartum mutant mothers had reduced oxytocin-positive neurons in the hypothalamus compared with the wild-type females (Fig. 4). The total number of oxytocin-positive neurons in the mutant females was 2984 ± 209 compared with 4496 ± 252 in the controls ($n = 5$, $P < 0.02$). The difference was significant even after allowing for the lower body weight and smaller PVN size in mutant females (Fig. 4). The reduced weight gain of pups could therefore be explained by an insufficient oxytocin surge.

In rodents, central oxytocin synthesis increases at parturition, and central infusions of this hormone stimulate a rapid maternal behavior (*18*), but this behavior is inhibited by the hormone antiserum or antagonists (*19*). Thus, the behavioral and neuroendocrine responses in this study have oxytocin as a common component for both the peripheral and central events that are impaired in the *Peg3*$^{\beta geo}$ mutants. The reduced number of oxytocin-producing neurons may have impaired the neuronal coupling and synchrony, which is required for a bolus of oxytocin release at postpartum to achieve milk letdown (*20*). The involvement of Peg3 in the TNF signaling pathway affecting cell survival and proliferation (*8*) could account for these decreases in oxytocin neurons in the PVN and other hypothalamic neurons. However, this major endocrine dysfunction cannot explain the behavioral phenotype fully, because *Peg3* mutant mothers conceived normally, gave birth, and had normal development of mammary glands during lactation.

There are now two imprinted genes, *Peg3* and *Mest* (*4*), of different structural classes implicated in the behavioral function of the CNS. This suggests that maternal behavior may be a specifically selected function through imprinting of neurally expressed genes. The most widely accepted hypothesis for genomic imprinting is that of "parental conflict," in which the parental genomes compete to regulate intrauterine embryonic growth through different sets of imprinted genes (*21*). Maternal behavior is a powerful motivation that is essential for the survival of offspring, which is governed by the hypothalamus. However, for females to maximize their lifetime reproductive success, it is necessary for progression to the next pregnancy to happen in the shortest possible time. While nursing the young, female rodents can mate at postpartum estrus and allow embryonic development to continue to the blastocyst stage when they enter into diapause (*22*). At the end of lactation, these embryos implant and continue development. Lactation and pregnancy (involving embryonic growth) demand considerable maternal energy resources; these two demands cannot be met simultaneously. Because the paternal interest is best served by prolonged care and feeding of his progeny through maternal lactation, there are asymmetrical parental interests involved. This could explain why the paternal genome may have acquired the ability to regulate maternal behavior through imprinted genes such as *Mest* and *Peg3*.

References and Notes

1. J. McGrath and D. Solter, *Cell* **37**, 179 (1984); M. A. H. Surani, S. C. Barton, M. L. Norris, *Nature* **308**, 548 (1984).
2. B. M. Cattanach and C. V. Beechey, in *Genomic Imprinting*, R. Reik and A. Surani, Eds. (Oxford Univ. Press, New York, 1997), pp. 118–141; R. Fundele, M. Surani, N. Allen, in *Genomic Imprinting*, R. Reik and A. Surani, Eds. (Oxford Univ. Press, New York, 1997), pp. 98–112.
3. E. B. Keverne, R. Fundele, M. Narasimha, S. C. Barton, M. A. Surani, *Dev. Brain Res.* **92**, 91 (1996).
4. T. Kaneko-Ishino *et al.*, *Nature Genet.* **11**, 52 (1995); L. Lefebvre *et al.*, *ibid.* **20**, 163 (1998).
5. Y. Kuroiwa *et al.*, *ibid.* **12**, 186 (1996).
6. F. Relaix *et al.*, *Dev. Biol.* **177**, 383 (1996).
7. J. Kim, L. Ashworth, E. Branscomb, L. Stubbs, *Genome Res.* **7**, 532 (1997).
8. F. Relaix, X. J. Wei, X. W. Wu, D. A. Sassoon, *Nature Genet.* **18**, 287 (1998).
9. The gene structure and restriction map of *Peg3* were determined in genomic clones isolated from 129Sv-derived genomic libraries (L.-L. Li *et al.*, unpublished observations). A 12.5-kb *Peg3* plasmid clone pB, spanning exons 3 to 9, contains two Xho I sites (one within exon 5 and the other at the 3′ cloning site in the plasmid) and two Hind III sites (one within exon 9 and the other within the plasmid backbone). A 4.8-kb IRES-β*geo*-SV40 polyadenylation selection cassette was isolated from pIFS (provided by J. Dixon) after Xho I digestion. A targeting vector was generated by deleting the 3′ 2.4-kb Hind III fragment from pB, followed by insertion of the cassette into the remaining single Xho I site in exon 5, in the same transcription direction as *Peg3*. R1 embryonic stem (ES) cells were electroporated with Not I–linearized targeting vector (50 μg), subjected to positive (G418, 150 μ/ml) selection, and screened by Southern (DNA) blot hybridization. 5′ and 3′ probes detected a 14.5-kb Hind III band and a 17-kb Bgl II band from the mutant locus and a 23-kb Hind III band and a 12-kb Bgl II band from the wild-type locus, respectively (Fig. 1A). Mutant ES clones were injected into MF1 blastocysts, and germ line chimeric males were mated to both wild-type 129Sv and MF1 females. Two ES clones showed identical phenotypes on the 129Sv background in this study. Progeny were genotyped by Southern hybridization or by polymerase chain reaction (PCR) with the following primer pairs: A (CAACAGTGACATGAACAGTG) and B (ATCGAGACTCATAATCCATG), which are specific to exons 4 and 5 of *Peg3* and flank the β*geo* cassette in the mutant locus, and C (GGGTGGAGAGGCTATTCGGCTAT) and D (GAAGAACTCGTCAAGAAGGCGATAGAA), which are specific for *neo*. β-Gal was expressed only upon paternal transmission of the mutant locus (Fig. 1C), which allowed us to distinguish the parent of origin of the mutant locus in heterozygous mice.
10. Northern (RNA) blot analyses with a *Peg3* cDNA probe located 3′ to the β*geo* integration site detected a very weak signal in the +/– and –/– embryos after a long exposure of the blots (Fig. 1B). Further reverse transcription PCR analysis showed that this signal was an aberrant alternatively spliced transcript involving exon 4, 49 nucleotides from the β*geo* cassette and exon 6. No wild-type *Peg3* transcript was detectable from the normally silent maternal allele in these embryos. As this residual aberrant transcription deleted exon 5 and introduced translation stop codons in the open reading frame, it is most likely that paternal transmission of this mutation would diminish the function of *Peg3*. Indeed, the mutant embryos predominantly expressed a 5.5-kb transcript, as detected with a 5′ fragment of β*geo* (Fig. 1B). The size of this transcript agrees with the termination of the *Peg3*-β*geo* fusion transcript at the simian virus 40 (SV40) polyadenylation site.
11. The mutant embryos and placentas were significantly growth retarded at 17.5 days post coitum [1.008 ± 0.023 g ($n = 25$) compared with 1.179 ± 0.024 g ($n = 27$, $P < 0.01$) and 0.069 ± 0.002 g ($n = 20$) compared with 0.096 ± 0.003 g ($n = 18$, $P < 0.01$), respectively] but without any discernible histological abnormality. At birth, the mutants were 81% of the normal weight, and this figure declined to 65% by 4 weeks of age. The major organs in the mutants, although proportionally smaller, were morphologically normal.
12. G. Calamandrei and E. B. Keverne, *Behav. Neurosci.* **108**, 113 (1994).
13. E. Noirot, *Anim. Behav.* **17**, 542 (1969); R. Gandelman, *Horm. Behav.* **4**, 257 (1973).
14. Brains were cryosectioned at 15 μm, fixed in 4% paraformaldehyde in phosphate-buffered saline (PBS) at 4°C for 5 min, and subjected to in situ hybridization as described [N. Kikyo *et al.*, *Dev. Biol.* **190**, 66 (1997)]. A 3.8-kb *Peg3* cDNA clone CS46 (*5*) was used to prepare sense and antisense probes with the digoxigenin RNA labeling kit (Boehringer Mannheim).
15. M. Numan, *Acta Paediatr. Suppl.* **397**, 19 (1994).
16. J. R. Brown, H. Ye, R. T. Bronson, P. Dikkes, M. E. Greenberg, *Cell* **86**, 297 (1996).
17. I. Scott *et al.*, *J. Neuroendocrinol.* **8**, 847 (1996); K. Nishimori *et al.*, *Proc. Natl. Acad. Sci. U.S.A.* **93**, 11699 (1996).
18. J. D. Caldwell, E. R. Greer, M. F. Johnson, A. J. Prange Jr., C. A. Pedersen, *Neuroendocrinology* **46**, 39 (1987); C. A. Pedersen and A. J. J. Prange, *Proc. Natl. Acad. Sci. U.S.A.* **76**, 6661 (1979).
19. E. van Leengoed, E. Kerker, H. H. Swanson, *J. Endocrinol.* **112**, 275 (1987); M. M. McCarthy, *Horm. Behav.* **24**, 365 (1990).
20. G. I. Hatton, Q. Z. Yang, P. Cobbett, *Neuroscience* **21**, 923 (1987).
21. T. Moore and D. Haig, *Trends Genet.* **7**, 45 (1991).
22. J. F. Bellringer, H. P. Pratt, E. B. Keverne, *J. Reprod. Fertil.* **59**, 223 (1980); A. P. F. Flint, M. B. Renfree, B. J. Weir, *J. Reprod. Fertil.* (suppl., 29 (1981).
23. β-Gal staining was performed as described [C. Bonnerot and J.-F. Nicolas, *Methods Enzymol.* **225**, 451 (1993)]. Briefly, embryos or tissues were fixed in 2% formaldehyde/0.2% glutaraldehyde in PBS at 4°C for 1 to 2 hours and incubated in PBS containing X-gal (1 mg/ml), 4 mM $K_4Fe(CN)_6$-$3H_2O$, 4 mM $K_3Fe(CN)_6$, 2 mM $MgCl_2$, and 0.02% NP-40 at 30°C in the dark until the color developed. The samples were postfixed in 4% formaldehyde and dehydrated in 70% ethanol. For cryosection, tissues were fixed in 4% formaldehyde/PBS, equilibrated in 30% sucrose in PBS at 4°C overnight, and cryosectioned at 15 nm. These sections were stained with X-gal solution, postfixed, and counterstained with nuclear fast red or eosin.
24. Age-matched wild-type and mutant females were subjected to maternal behavior as described [J. A. G. Yeo and E. B. Keverne, *Physiol. Behav.* **37**, 23 (1986)]. The females were individually housed and presented with three newborn pups, which were placed separately opposite to their nest site and with nest materials moved to the center of the cage. The responses of females were recorded for 30 min as follows. (i) Retrieval: The female picked up a pup and transported it to her nest site. (ii) Nest building: The female brought nest materials to her nest site. (iii) Crouching over pups: The female covered the three pups and arched her back in a nursing posture.
25. Mice were anesthetized and perfused with cold 4% paraformaldehyde in PBS. Brains were dissected, postfixed overnight, equilibrated in 30% sucrose at 4°C overnight, and cryosectioned at 40 μm. Sections were incubated at room temperature overnight with polyclonal antisera to oxytocin (Cambridge Bioscience). The binding of antibody was detected with the ABC technique (Vectastain).

26. We are very grateful to the members in our laboratories, in particular, J. F.-X. Ainscough and R. John for their valuable comments on this manuscript. The work was supported by grants from the Wellcome Trust and Human Frontier Science Program to M.A.S.

18 December 1998; accepted 12 March 1999